

# The Use of Overpressure in Thermolytic Debinding of Moulded Ceramic Bodies

P. D. Hammond & J. R. G. Evans

Department of Materials Technology, Brunel University, Uxbridge, Middlesex, UK, UB8 3PH

(Received 18 April 1994; revised version received 3 June 1994; accepted 30 June 1994)

## Abstract

*A furnace within a pressure vessel capable of withstanding 0–1 MPa and temperatures up to 600°C is described. The furnace allows the pyrolysis of injection moulded ceramics to take place at higher heating rates than is possible at atmospheric pressure without defects caused by bloating or cracking. The effectiveness of the method is described for a commercial injection-moulding composition pyrolysed in nitrogen. The various effects of gas pressure on the process are listed and the main beneficial effect is considered to be the increase in boiling point of the polymer-degradation product solution which forms the continuous phase. In the early stages of heat treatment, this allows more rapid mass transport both by diffusion and fluid flow.*

## 1 Introduction

Many techniques drawn from polymer processing have been successfully applied to ceramic suspensions in order to facilitate the arrangement of particles into complex shapes before firing.<sup>1</sup> The most versatile of these is injection moulding, but they all have the disadvantage that organic matter initially filling the interstitial space must be removed before firing. This presents particular problems for thick sections made by injection moulding.

Capillary<sup>2</sup> and solvent<sup>3</sup> methods have been used for binder removal but the most popular method is pyrolysis either in an oxidative atmosphere,<sup>4</sup> an unreactive atmosphere<sup>5</sup> or in vacuo.<sup>6</sup> Frequently mouldings are packed in a powder bed during heat treatment and loss of molten organic vehicle is assisted by partitioning between the two powder assemblies. During pyrolysis, three weight loss processes can be identified, dependent on ambient atmosphere and molecular weight of the organic vehicle.<sup>7</sup> For low molecular weight material, evap-

oration proceeds without chain scission and the thermogravimetric characteristics are little affected by atmosphere. For high molecular weight organic vehicles, chain scission must precede evaporation and this can occur either by oxidative degradation, in which case it is likely to be affected by the diffusion of oxygen into the body,<sup>8</sup> or by thermal degradation, in which case it will occur uniformly throughout the body if the degradation reaction is irreversible.

Under oxidising atmospheres the former reaction predominates, although under conditions of prolonged heating, such as those needed for binder removal from thick sections, thermal degradation will proceed to some extent in all cases. Thermal degradation therefore deserves priority of attention because low molecular weight products of decomposition are formed throughout the body at a stage when interconnected porosity is absent.

A manufacturer often wishes to minimise the debinding time in order to reduce the number of stationary semi-finished products. Low-temperature furnace costs are modest and debinding times often compare favourably with raw material bulk storage times so that the debinding stage does not incur such a prohibitive debit as is sometimes claimed. The main benefit of shortening this stage accrues if the lead time for new products can be reduced. Another advantage of enhancing the debinding stage is that larger sections may be successfully treated in sensible time scales.

Several strategies are available under this objective. The organic vehicle can be selected to decompose steadily as temperature rises.<sup>9,10</sup> The process can be controlled by an external loop so that weight loss is a linear function of temperature.<sup>11</sup> The organic vehicle can be synthesised to have the combined properties needed to prevent the boiling of degradation products in solution.<sup>12</sup> Pressure can be applied to the decomposing system.<sup>13</sup> This work explores the latter intervention.

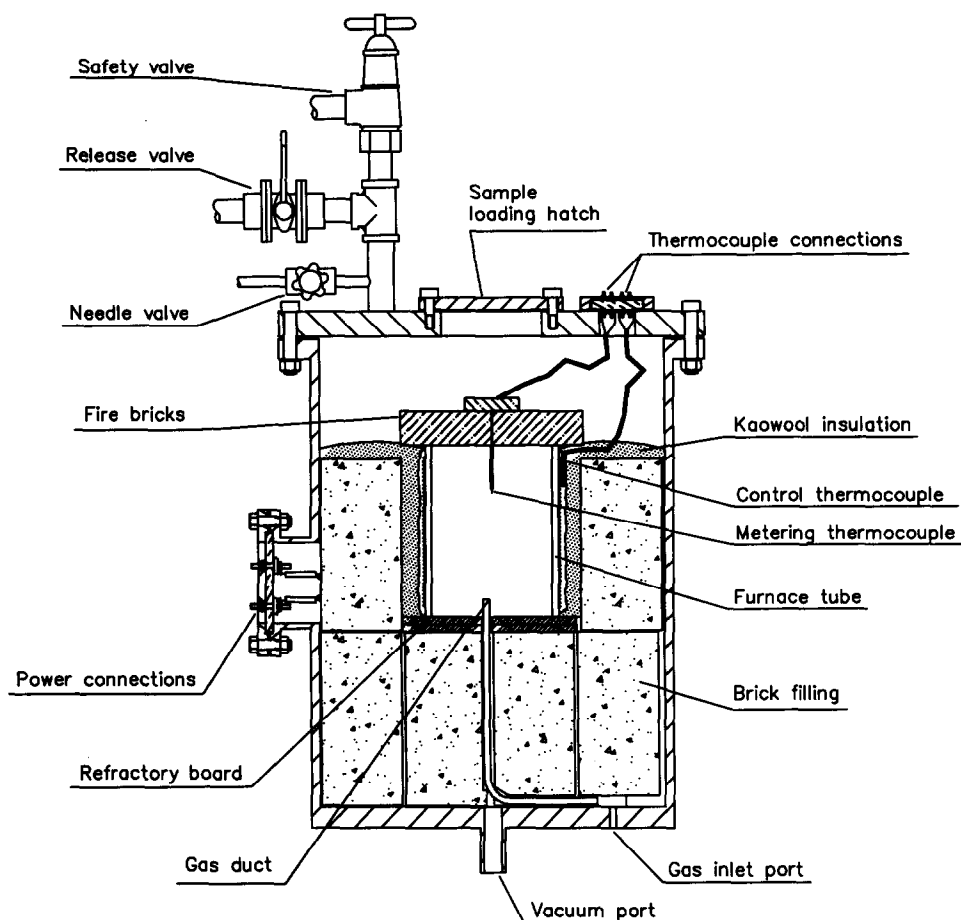


Fig. 1. Diagram of the pressure vessel and furnace.

## 2 Experimental Details

### 2.1 Furnace design

The pressure vessel was manufactured from carbon-manganese steel to the specifications of BS1500, which has recently been superseded by BS5500.<sup>14</sup> Its internal dimensions were 435 mm diameter  $\times$  600 mm in height. This allows a large furnace to be incorporated or alternatively a series of small furnaces. The present work was carried out with a 150 mm diameter  $\times$  200 mm furnace wound from 80/20 Ni/Cr wire on a silica glass tube. Figure 1 shows the vessel and furnace diagrammatically. The top, wall and base were water-cooled by independent circuits incorporating flow indicators. Wall temperature was monitored by three series-connected thermal switches (opening at 40°C) which latched a relay controlling electric power to the furnace. Oxygen-free nitrogen was used in all the experiments. A preset Nabic spring-operated safety valve was fitted to prevent the rated working pressure of 1.05 MPa being exceeded. Gas throughput was controlled by a needle valve venting through a flow meter into an oil indicator. Electric leadthroughs were made through 20 mm thick discs of cloth-reinforced phenol-formaldehyde resin (Tufnol, Birmingham, UK) clamped with O-ring seals. The internal and

external surfaces of the vessel were treated with a two-part organic-resistant epoxy-based paint (Trimite, Uxbridge, UK). The general arrangement of the furnace vessel and its ancillary circuits are shown in Fig. 2.

A Eurotherm 818P temperature controller was used to provide linear heating rates and the controller thermocouple, mounted on the outside of the windings, was calibrated dynamically against the hot zone thermocouple at three gas pressures, 0.1, 0.6 and 1.0 MPa, and for each sample container. The procedure for filling the vessel involved evacuation to about 2.5 kPa followed by filling with oxygen-free nitrogen. A gas flow of  $10^{-6} \text{ m}^3 \text{ s}^{-1}$  was maintained during experiments and the internal pipework allowed the gas to enter at the base of the furnace tube. Although the oxygen content of the nitrogen was not measured directly, the furnace was heated to 600°C with copper powder and the weight changes indicated that negligible oxidation had taken place. Significant polymer oxidation may therefore also be assumed to be absent.

### 2.2 Materials and mouldings

The ceramic powder was a proprietary silica ( $<200 \mu\text{m}$ ) having a density of  $2200 \text{ kgm}^{-3}$ , used for leachable foundry cores for nickel alloy tur-

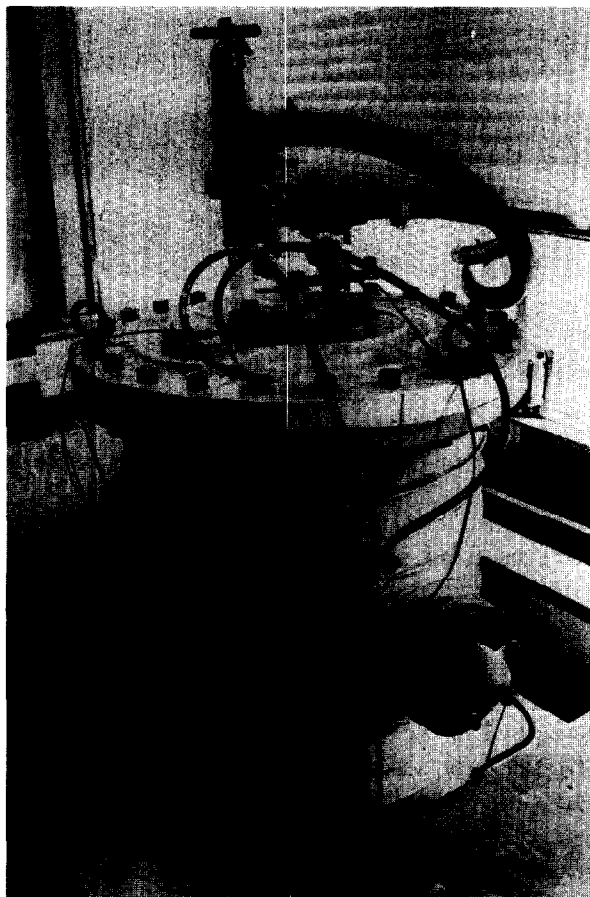


Fig. 2. The pressure vessel showing the arrangement of valving and coolant.

bine blades. The organic vehicle was a proprietary blend based on a low molecular weight polyethylene glycol diluted with waxes and a stearate as a processing aid and had a density of  $1110 \text{ kgm}^{-3}$ . Ashing showed a 22.1% weight loss indicative of a powder loading of 64 vol.%. Injection moulding of 17 mm diameter cylinders, 100 mm in length was performed at Fairey Tecramics Ltd using a Florin injection-moulding machine with a maximum barrel temperature of  $60^\circ\text{C}$  and a maximum injection pressure on material of 52 MPa. The cylinders were contact radiographed before pyrolysis using a Hewlett Packard Faxitron camera. A Perkin Elmer TMA dilatometer with a flat-ended silica rod and a 10 g load was used to determine the dilatometric softening point of the suspension. Thermogravimetry was performed on a Perkin Elmer (Beaconsfield, Bucks, UK) model TGS2.

### 2.3 Pyrolysis

Three methods of sample support were used. Some samples were placed on a refractory tile with a dusting of coarse alumina (Grade LG20, Alcan Chemicals, UK). Others were fully packed in this alumina powder, either in a steel trough or a ceramic crucible. In the third series of experiments, samples were packed in coarse SiC powder (Grade C6, Bescor Abrasives Ltd, Surrey, UK).

Tests were done at gas pressures of 0.1, 0.6 and 1.0 MPa. After heat treatment, the samples were lightly sintered to facilitate handling, by heating to  $1150^\circ\text{C}$ , holding for 4 h and furnace cooling. They were then examined externally, radiographed and cut across the central lateral cross-section to establish integrity. On certain samples, measurements of the horizontal and vertical diameters were taken at the centre of the bar, to find the ovality. Positive ovality (the difference between the horizontal diameter and the vertical diameter) was taken as an indication of the degree of slumping which had occurred. Linear heating from  $70^\circ\text{C}$  to  $500^\circ\text{C}$  was used throughout, with a ramp of  $60^\circ\text{C h}^{-1}$  from  $20^\circ\text{C}$  to  $70^\circ\text{C}$  and from  $500^\circ\text{C}$  to room temperature.

### 3 Results and Discussion

Although it is routine practice to carry out a steady-state furnace calibration, what is required here is a dynamic calibration because the integrity of samples is assessed in terms of a critical heating rate. The hot zone temperature initially lags behind the set temperature but the hot zone rate increases as temperature rises, producing families of calibration curves such as that shown in Fig. 3.

At the low heating rates typical of thermolytic debinding at atmospheric pressure, the rates coincide over the range of temperatures of interest. The high rates of heating that are possible under overpressure conditions, however, may lead to substantial deviations. The choice of temperature at which to deduce the actual rate is fixed by the initial region of rapid thermal degradation and may be deduced from appropriate thermogravimetric curves. Since the thermogravimetric loss behaviour varies with heating rate, the problem is to decide at which temperature to convert set rate to actual rate. The procedure used here was to select the temperature at which an arbitrary 20wt% loss based on the initial weight of binder had occurred.

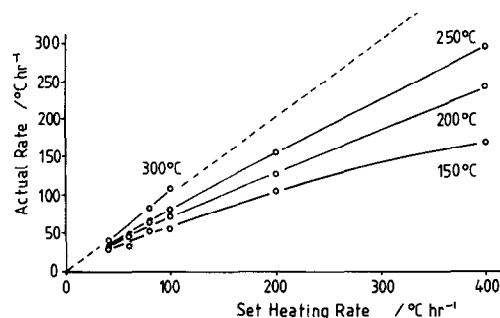


Fig. 3. An example of the dynamic calibration for heating rate at various hot zone temperatures. (0.6 MPa, setter powder LG20 alumina in stainless steel trough.) The dashed line represents set rate = actual rate.

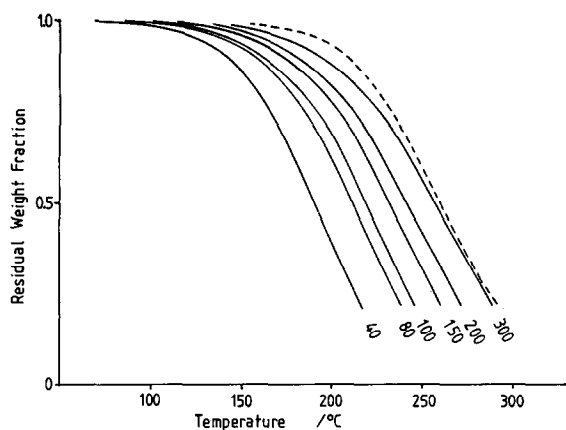


Fig. 4. Thermogravimetric curve for the organic vehicle heated in nitrogen at 300°C h<sup>-1</sup> (dashed line) and calculated curves for other heating rates labelled on the curves in °Ch<sup>-1</sup>.

From the thermogravimetric loss curve at a rate of 300°C h<sup>-1</sup> the activation energy  $E$  and specific rate constant  $K_0$  were obtained by the method of Wendlandt.<sup>15</sup> This makes the assumption that the weight loss is a first order reaction and therefore neglects the effect of evaporation of low molecular weight additives which are lost by zero order kinetics. It does not attempt to assess the loss of fluid by partitioning into the porous powder support.

The reaction is therefore treated as obeying

$$\frac{dw}{dt} = -Kw \quad (1)$$

where  $w$  is the weight fraction of binder remaining and  $K$  is the rate constant which varies with temperature as

$$K = K_0 \exp\left(\frac{-E}{RT}\right) \quad (2)$$

Once  $K_0$  and  $E$  are known, the thermogravimetric loss curve can be constructed for any heating rate  $Z$  using

$$w = \exp\left\{-K_0 \frac{RT^2 \exp(-E/RT)}{ZE}\right\} \times \left[1 - \frac{2RT}{E} + \frac{6(RT)^2}{E^2}\right] \quad (3)$$

Figure 4 shows the experimental thermogravimetric curve at a rate of 300°C h<sup>-1</sup>, together with the curve recalculated using eqn (3). This method inevitably results in some error because the activation energy plot is linear over a restricted range of temperature; in this case 212° to 276°C.

The corresponding curves for other heating rates are also shown. This is an approximate way of executing the rate calibration and the errors are most pronounced at high set rates. Both set and calculated heating rates are quoted for overpressure experiments in Tables 1–3.

The bars were radiographed to ensure that they

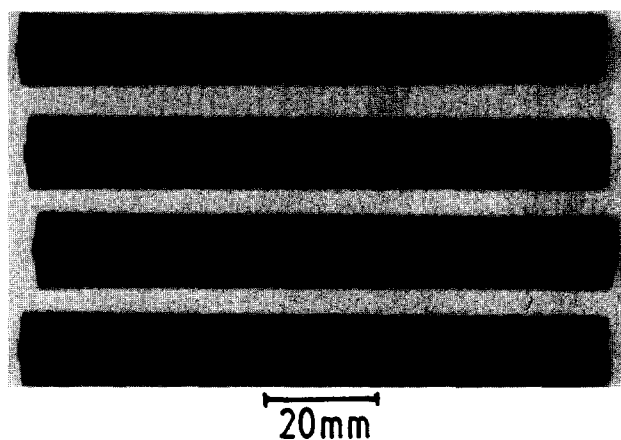


Fig. 5. Prints of radiographs of moulded bars before heat treatment.

were free from shrinkage voids or cracks caused by the injection-moulding processes which might interfere with the assessment of critical heating rate. In general the bars were free from such defects and examples of prints of radiographs are shown in Fig. 5.

In the first series of experiments, the samples were supported on a refractory tile with a thin layer of alumina powder. The results are summarised in Table 1. This identifies three factors influencing the quality of moulding after binder removal. The effect of heating rate is seen by comparing samples heated at set rates of 5°C h<sup>-1</sup> and 15°C h<sup>-1</sup>, showing that the critical heating rate at atmospheric pressure lies between these temperatures. The sample heated at a set rate of 5°C h<sup>-1</sup> is shown in Fig. 6. Samples heated at a set rate of 40°C h<sup>-1</sup> under 0.6 MPa pressure, although defective in cross-section, were only marginally worse than the sample heated at 15°C h<sup>-1</sup> under 0.1 MPa, indicating that overpressure has a beneficial effect. Samples heated at set rates of 100 and 200°C h<sup>-1</sup> showed severe deformation due to

Table 1. Integrity of mouldings heat treated on a tile, unsupported by powder

Heating rate °Ch <sup>-1</sup>		Pressure (MPa)	Results
Set	Actual		
5	5	0.1	No surface cracks, no visible defects in cross-section
15	13	0.1	No surface cracks, signs of slight internal cracking
20	18	0.6	Some surface cracks, signs of internal cracking
40	35	0.6	Some surface cracks, signs of internal cracking
100	83	0.6	Extensive surface cracks and parallel cracks in section, extensive slumping
200	180	0.6	Extensive surface cracks and parallel cracks in section, extensive slumping

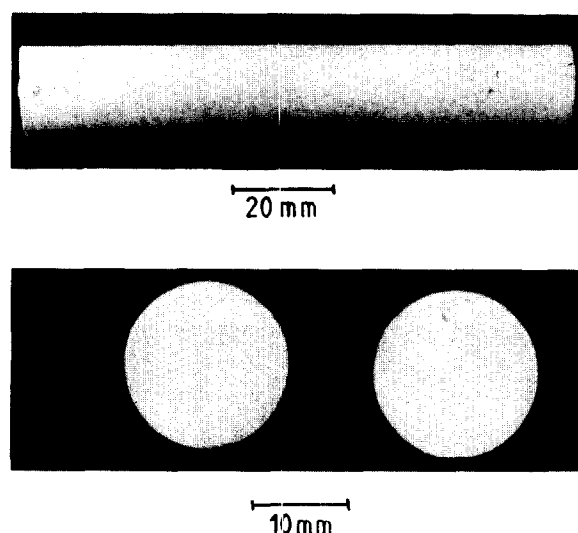


Fig. 6. Sample heated on a tile at a set rate of  $5^{\circ}\text{C h}^{-1}$  at atmospheric pressure.

slumping and the cracks in the cross-section were perpendicular to the direction of deformation. This highlights the sample support as a relevant variable; an issue that does not arise at lower heating rates (Fig. 6). It follows that the interaction of the supporting medium with the component during pyrolysis must also be assessed.

Figure 7 shows the outer appearance and cross-sections of the sample heated at  $200^{\circ}\text{C h}^{-1}$  on the refractory tile. Although the rate is well above critical for this condition, much of the damage is associated with the deformation. The extent of sagging is measured by ovality and plotted as a function of heating rate in Fig. 8 for samples resting on a shallow bed of powder (curve A) and for samples fully embedded in powder (curve B). For heating rates which could be used at atmospheric pressure, slumping does not occur. This is because the deformation of moulded ceramics is sensitive to ceramic volume loading and when sufficient

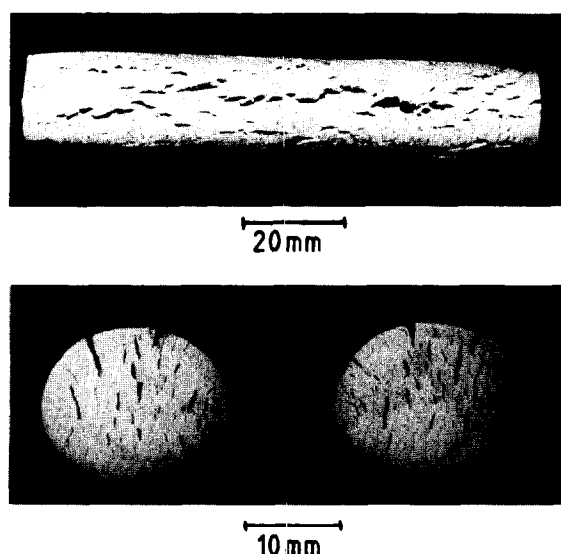


Fig. 7. Slumping caused by inadequate support during heating at a set rate of  $200^{\circ}\text{C h}^{-1}$  at 0.6 MPa.

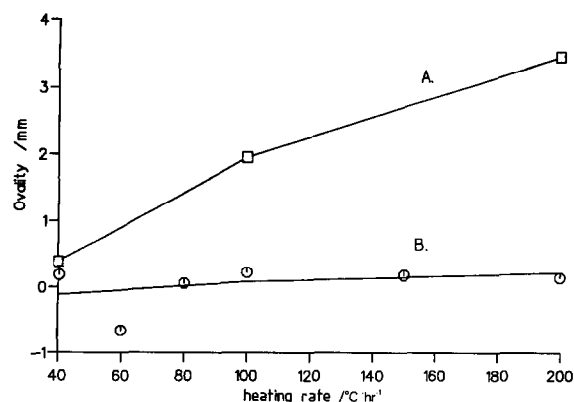


Fig. 8. The effect of sample support on deformation due to slumping. A: Samples resting on shallow powder bed. B: Samples packed inside powder bed.

binder has been displaced, the suspension acquires quasi-solid properties.<sup>16</sup> Under circumstances where an overpressure permits the use of higher heating rates, the thermogravimetric weight loss curve is displaced to higher temperatures.<sup>17</sup> The organic phase then has lower viscosity and, due to differential thermal expansion, occupies a higher volume fraction, so that flow is enhanced. Thus, when overpressure is employed, extra precautions are needed for component support.

The second series of experiments was therefore carried out with samples embedded in the alumina powder. As well as supporting the component, the powder bed may also contribute to safe debinding by capillary extraction when the organic vehicle is based on a low molecular weight system.<sup>18,19</sup> The amount of binder extracted in the molten state isothermally at  $130^{\circ}\text{C}$  after heating for 3 h and 19 h in the alumina powder was 21% and 69% respectively. A sample heated on an alumina tile for the same periods lost 1.4% and 6.1% respectively. Thus the alumina powder is effective in removing some of the organic vehicle by capillary extraction. However, the 19 h heat treatment considerably exceeds the time for which the binder was molten during pyrolysis under overpressure, which was typically less than 3 h at 0.6 MPa.

Figure 8 shows that shape was retained over the range of heating rates explored when a powder bed was used and this is reflected in the pattern of defects. Figure 9 shows a bar heated at a set rate of  $200^{\circ}\text{C h}^{-1}$  and 0.6 MPa, which should be compared with Fig. 7. The slumping is absent and the cracks are no longer unidirectional.

The results for samples embedded in alumina (Table 2) suggest that at 0.1 MPa the critical heating rate is not greatly increased by the presence of the powder bed. In the sample heated at a set rate of  $100^{\circ}\text{C h}^{-1}$  the effect of boiling of low molecular weight organic compounds in solution in the main polymer is clearly seen as bloating (Fig. 10). At this pressure the boiling occurs at a temperature

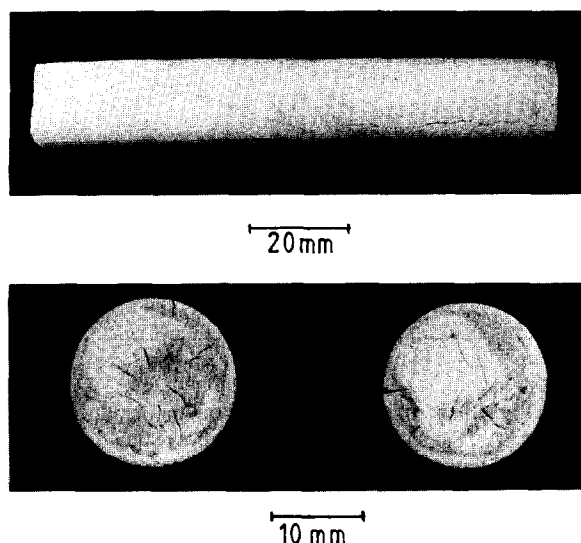


Fig. 9. Defects in a bar supported in an alumina powder bed and heated at a set rate of  $200^{\circ}\text{C h}^{-1}$  under 0.6 MPa.

where the suspension is fluid because little binder has been expelled; an effect resulting from the high heating rate. In subsequent work at higher pressures and similar heating rates the defects take the form of cracks because their initiation has been deferred to higher temperatures by the suppression of boiling and by that stage more binder has gone and the ceramic volume fraction is consequently higher.

At 0.6 MPa, the critical heating set rate is in the region  $80\text{--}100^{\circ}\text{C h}^{-1}$ . Figure 11, for example, shows the surface and sections of a bar heated at  $80^{\circ}\text{C h}^{-1}$ , which is of good quality. The use of a pressure of 1.0 MPa gave a sample free from in-

Table 2. Integrity of moulding heat treated in an alumina powder bed

Heating rate $^{\circ}\text{C h}^{-1}$		Pressure (MPa)	Results
Set	Actual		
20	18	0.1	Outer surface defect-free, slight internal cracking at centre
40	30	0.1	As above
100	70	0.1	Severe surface cracking, internal bloating
15	14	0.6	Free from macro-defects
40	32	0.6	Free from macro-defects
60	44	0.6	Free from macro-defects
80	60	0.6	Free from macro-defects
100	70	0.6	Slight surface cracking, slight internal cracking
150	100	0.6	Slight cracking, internal cracks
200	130	0.6	Surface cracking, internal cracking
100	63	1.0	No internal cracks, surface cracks due to loss of powder
125	75	1.0	Surface defect-free, very slight central cracks
150	95	1.0	Surface very slightly cracked, internal cracks
200	125	1.0	Surface cracks, internal cracks

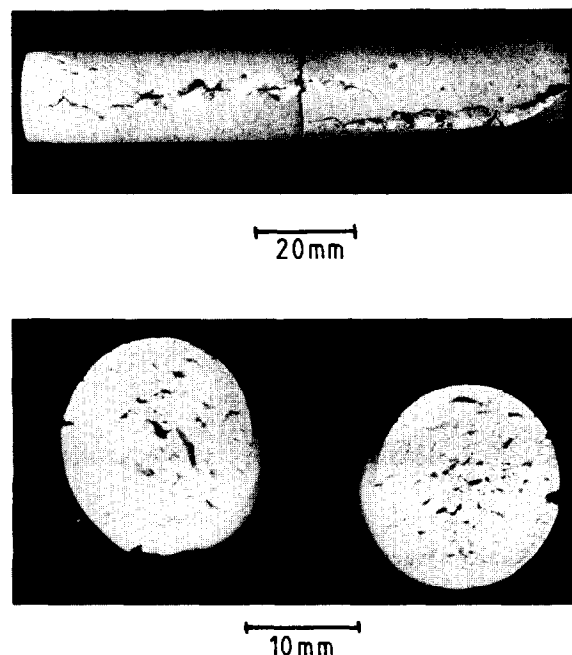


Fig. 10. Surface and sections of a bar heated at a set rate of  $100^{\circ}\text{C h}^{-1}$  under 0.1 MPa while supported in a powder bed. Defects at the centre take the form of bubbles resulting from boiling because at this heating rate the suspension retains fluidity.

ternal defects at a set rate of  $100^{\circ}\text{C h}^{-1}$  (actual rate  $63^{\circ}\text{C h}^{-1}$ ). This sample showed slight surface cracks on the top surface associated with loss of setter powder. Exposed surfaces generally presented this problem. The loss was caused by admitting nitrogen to the vessel at too high a rate. The use of 1 MPa overpressure did not give an improvement over the critical rate achieved at 0.6 MPa. Three reasons why the full benefit of overpressure may not be obtained in practice are discussed later.

The pressures used here do not present severe laboratory safety problems provided normal precautions are taken. The construction of the apparatus involved very modest capital expenditure.

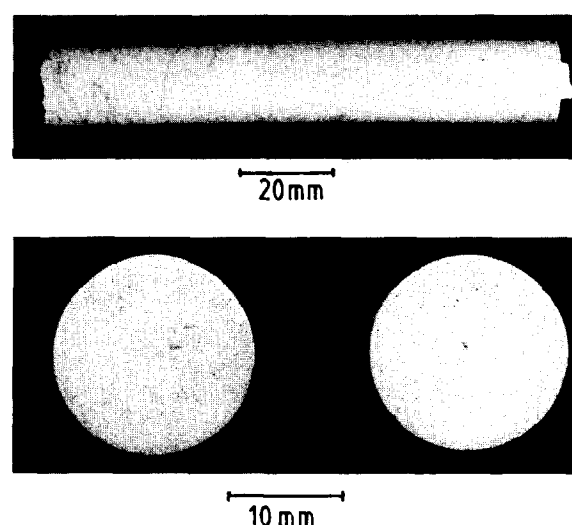


Fig. 11. Surface and sections of a bar heated at a set rate of  $80^{\circ}\text{C h}^{-1}$  under 0.6 MPa.

These factors imply that the widespread use of overpressure debinding is relatively unimpeded.

In order to understand the role of overpressure in a non-oxidising environment, one may enumerate the individual effects it may have on the system as follows:

- (1) Increase in the boiling point of low molecular weight constituents of the organic vehicle and of the solution of degradation products (as solute) in molten polymer (as solvent)
- (2) Decrease in diffusion coefficient of degradation product in solution caused by reduction in polymer free volume.<sup>20</sup>
- (3) Closure of pre-existing defects when the organic vehicle is molten.
- (4) Increase in vapour pressure of volatile species.
- (5) Dissolution of ambient gas in the molten polymer.
- (6) Increase in convective heat transfer in the furnace.
- (7) Influence on gaseous diffusion of degradation products in the porous region.
- (8) Changes in the distribution of degradation products.
- (9) Changes in miscibility of organic liquid mixtures.

These effects are assessed individually elsewhere<sup>21</sup> and arguments are presented to suggest that the first contribution is overriding. Thermal degradation, which occurs throughout a moulding, liberates low molecular weight products of decomposition which dissolve in the parent polymer. When the vapour pressure over this solution at any point reaches ambience, boiling occurs. The resulting defects may take the form of round 'voids' characteristic of boiling in a liquid and examples are shown in Fig. 10 in a sample heated at  $100^{\circ}\text{C h}^{-1}$  at atmospheric pressure. If, however, some polymer has already been lost, and hence ceramic volume fraction has risen, the suspension behaves as a solid,<sup>16</sup> even though continuous porosity has not yet formed. Defects then take the form of a crack. When the external pressure is raised, the boiling point is elevated and the system can reach higher temperatures without defects occurring. Mass transport processes which are thermally activated are then enhanced.

The critical stage in thermolytic debinding occurs in the early stages of degradation where most pores are filled. The suppression of boiling enhances the diffusion coefficient for degradation products migrating in solution in the continuous phase both by raising the temperature and by allowing a higher diffusant concentration to prevail. In free volume theory, both effects conspire to have a pronounced influence on diffusion.<sup>22</sup>

**Table 3.** Integrity of samples heated in a coarse SiC powder bed

Heating rate $^{\circ}\text{C h}^{-1}$		Pressure (MPa)	Results
Set	Actual		
20	16	0.6	{ Very slight internal cracking Outer surface defect free
40	30	0.6	
150	102	0.6	Some internal cracks
200	135	0.6	Many internal cracks
400	<sup>a</sup>	0.6	Surface and internal cracks, no slumping.

<sup>a</sup> Outside the range of calibration.

Secondly, by allowing the polymer to reach a higher temperature, viscosity is reduced and capillary flow into the surrounding powder is speeded up.<sup>19</sup> It is beyond the scope of this work to quantify the competition between these two transport processes but an indication of their relative importance can be found by using a powder which supports the sample against slumping but has negligible ability to extract the organic vehicle by capillary flow.

This comparison is shown in the third series of experiments in which coarse silicon carbide powder was used as the setter powder. In partitioning experiments, the amount of binder based on the initial weight in the sample after 3 h and 19 h in the SiC setter powder was identical, to within 1%, to the loss experienced by companion samples heated at  $130^{\circ}\text{C}$  on a tile.

Table 3 shows the result of experiments with the silicon carbide setter. The critical heating rate at 0.6 MPa is lower than that obtained in the alumina powder, indicating that capillary extraction is a significant transport path in the alumina setter powder. At 0.6 MPa the extent of damage in samples supported in silicon carbide powder was less than that seen in samples which were unsupported or heated without overpressure for comparable heating rates.

Three reasons can be discerned for the failure to obtain the full potential benefit of overpressure. In the first place, the use of a powder bed reduces the effective surface mass transport coefficient for gaseous products leaving the body because of the static boundary layer provided by the powder. If support is mandatory, as implied by the results in Fig. 8, it will tend to provide a resistance to gaseous transport away from the surface of mouldings. A second reason is that where liquid capillary flow is a significant transport path, the capillary pressure falls with an increase in temperature due to the reduction of the surface energy of polymers with increasing temperature.<sup>19</sup> These factors may explain why the high values of critical

heating rate found with the alumina setter at 0.6 MPa were not further enhanced at 1 MPa.

A third reason why the full benefit of overpressure may not be achieved in practice arises from the problem of pressure transmission to the core of a moulding throughout the decomposition region. Before the open porosity stage is reached, shrinkage of the core as polymer is lost must be accompanied either by collapse of the shell or by diffusion of nitrogen to the centre. Collapse of the outer shell may be impeded if the peripheral ceramic weight fraction rises towards  $V_{\max}$ , the weight fraction at which viscosity approaches infinity,<sup>16</sup> and this is likely to occur at an early stage and to be associated with the shrinkage due to binder removal. Pressure transmission may thus rely upon diffusion of dissolved gas in the continuous phase.

Closely related to the problem of pressure transmission is the possibility that elevated ambient pressure applied to mouldings in the molten state will cause defects to collapse. This possibility was investigated empirically for similar bars moulded with low injection pressure which contained injection-moulding voids.

Two such test bars, measuring 10 mm × 10 mm × 75 mm, were radiographed to confirm the presence of voids. They were then heated to 80°C in the pressure furnace under atmospheric pressure. The softening point of the material was determined by thermomechanical analysis to be 51°C. When that temperature had been attained, the pressure was increased as rapidly as possible to 1 MPa, and held while the samples were cooled. They were radiographed again, but showed no difference in the internal voids. It is possible that nitrogen had diffused through the material to fill the pores in the time it was being admitted to the vessel, as filling the chamber took about 90s, or that the applied pressure was insufficient to cause the necessary deformation.

Samples of the same material were heated to 130°C inside the pressure vessel and the gas pressure was raised to 1 MPa. They were then cooled to room temperature under pressure and, upon removal, promptly placed in a glass-fronted oven at 130°C. Very slight surface bloating could be detected on reheating, which did not appear on samples reheated without overpressure treatment, indicating the presence of dissolved gas in the continuous phase.

#### 4 Conclusions

The use of modest overpressure (0–1 MPa) significantly increased the critical rate of heating of

commercial injection-moulded ceramics. The main benefit is considered to result from an increase in boiling point of the binder components and their degradation products in solution. This means that higher temperatures can be reached before boiling in the continuous phase occurs. At higher temperatures, mass transport by diffusion through the continuous phase and liquid flow into a surrounding powder are both enhanced.

When the higher heating rates made possible by overpressure are used, the sample must be supported against slumping, a requirement that does not prevail at low rates of heating for the samples tested here.

#### Acknowledgements

The authors are grateful to the Science and Engineering Research Council for a studentship for PDH and to Fairey Tecramics for jointly supporting this work. Thanks are due to Mrs K. Goddard for typing the manuscript.

#### References

1. Evans, J. R. G., Plastic forming operations for ceramic suspensions. In *New Materials and their Applications*, ed. D. Holland. Institute of Physics, UK, 1990, pp. 43–52.
2. Patterson, B. R. & Aria, C. S., Debinding injection-moulded materials by melt wicking. *JOM*, **41** (1989) 22–24.
3. Johnson, K. P., Metal injection by the InjectAMAX process. In *Advances in Powder Metallurgy 1989* Vol. 3. ed. T. G. Gasbarre & W. F. Jandeska. Metal Powder Industries Federation, NJ, USA, 1989, pp. 17–24.
4. Gilissen, R. & Smolders, A., Binder removal from injection moulded ceramic bodies. *Mater. Sci. Monog., High Technology Ceramics*, pt A, **38A** (1987) 591–4.
5. Mizuno, S., Binder removal from ceramic injection moulded bodies. JP Patent 61117 116 A2, 4 June 1986.
6. Mann, D. L., Injection moulding of sinterable, silicon base non-oxide ceramics. *Air Force Laboratory Technical Report AFML-TR-78-200*, December 1978.
7. Wright, J. K., Evans, J. R. G. & Edirisinghe, M. J., Degradation of polyolefin blends used for ceramic injection moulding. *J. Amer. Ceram. Soc.*, **72** (1989) 1822–8.
8. Wright, J. K. & Evans, J. R. G., Kinetics of the oxidative degradation of ceramic injection moulding vehicle. *J. Mater. Sci.*, **26** (1991) 4897–903.
9. Saito, K., Tanaka, T. & Hibino, T., UK Patent 1426317 25 February 1976.
10. Stedman, S. J., Evans, J. R. G. & Woodthorpe, J., A method for selecting organic materials for ceramic injection moulding. *Ceramics International*, **16** (1990) 107–13.
11. Johnsson, A., Carlstrom, E., Hermansson, L. & Carlsson, R., Minimisation of the extraction time for injection moulded ceramic. *Proc. Brit. Ceram. Soc.*, **33** (1983) 139–47.
12. Matar, S. A., Evans, J. R. G., Edirisinghe, M. J. & Twizell, E. H., The influence of monomer and polymer properties on the removal of organic vehicle from ceramic and metal mouldings. To be published.
13. Katagiri, T., Dewaxing furnace for technical ceramics. *Powder Metallurgy International*, **22** (1990) 37–9.



14. BS 5500, *Unfired fusion-welded pressure vessels*. British Standards Institution, London, UK, 4th revision, 1991.
15. Wendlandt, W. W., *Thermal Method of Analysis*. Wiley Interscience, NY, 1964, pp. 32–4.
16. Wright, J. K., Edirisinghe, M. J., Zhang, J. G. & Evans, J. R. G., Particle packing in ceramic injection moulding. *J. Amer. Soc.*, **73** (1990) 2653–8.
17. Coates, A. W. & Redfern, J. P., Thermogravimetric analysis. *Analyst*, **88** (1963) 906–24.
18. Wright, J. K. & Evans, J. R. G., Removal of organic vehicle from moulded ceramic bodies by capillary action. *Ceramics International*, **17** (1991) 79–87.
19. Bao, Y. & Evans, J. R. G., Kinetics of the capillary extraction of organic vehicle from ceramic bodies. II. Partitioning between porous media. *J. Eur. Ceram. Soc.*, **8** (1991) 329–38.
20. Ferry, J. D., *Viscoelastic Properties of Polymers*, Wiley, NY, 3rd edn, pp. 285–98.
21. Hammond, P. D., Thermolytic debinding of ceramic injection mouldings using overpressure. To be published.
22. Vrentas, J. S. & Duda, J. L., Diffusion. In *Encyclopedia of Polymer Science and Engineering*, Vol. 5, ed. J. I. Kroshwartz *et al.* Wiley, NJ, 1986, pp. 36–8.